Calculation of β-decay rates in a relativistic model with momentum-dependent self-energies

T. Marketin and D. Vretenar
Physics Department, Faculty of Science, University of Zagreb, Croatia, and Physik-Department der Technischen Universität München, D-85748 Garching, Germany

P. Ring
Physik-Department der Technischen Universität München, D-85748 Garching, Germany
(Received 14 December 2006; published 15 February 2007)

The relativistic proton-neutron quasiparticle random phase approximation (PN-RQRPA) is applied in the calculation of β-decay half-lives of neutron-rich nuclei in the $Z \approx 28$ and $Z \approx 50$ regions. The study is based on the relativistic Hartree-Bogoliubov calculation of nuclear ground states, using effective Lagrangians with density-dependent meson-nucleon couplings, and also extended by the inclusion of couplings between the isoscalar meson fields and the derivatives of the nucleon fields. This leads to a linear momentum dependence of the scalar and vector nucleon self-energies. The residual QRPA interaction in the particle-hole channel includes the $\pi + \rho$ exchange plus a Landau-Migdal term. The finite-range Gogny interaction is employed in the $T = 1$ pairing channel, and the model also includes a proton-neutron particle-particle interaction. The results are compared with available data, and it is shown that an extension of the standard relativistic mean-field framework to include momentum-dependent nucleon self-energies naturally leads to an enhancement of the effective (Landau) nucleon mass, and thus to an improved PN-QRPA description of β^--decay rates.

DOI: 10.1103/PhysRevC.75.024304 PACS number(s): 21.30.Fe, 21.60.Jz

Weak-interaction processes in exotic nuclei far from stability play an important role in stellar explosive events. In particular, β-decay rates of very neutron-rich nuclei set the time scale of the r-process nucleosynthesis, i.e., the multiple neutron capture process which determines the synthesis of nearly half of the nuclei heavier than Fe. Since the vast majority of nuclides which lie on the path of the r-process will not be experimentally accessible in the foreseeable future, it is important to develop microscopic nuclear structure models that can provide accurate predictions of weak-interaction rates of thousands of nuclei with large neutron to proton asymmetry. There are basically two microscopic approaches that can be employed in large-scale calculations of β-decay rates: the interacting shell model and the quasiparticle random phase approximation (QRPA). While the advantage of using the shell model is the ability to take into account the detailed structure of the β-strength function [1], the QRPA approach is based on global effective interactions and provides a systematic description of β-decay properties of arbitrarily heavy nuclei along the r-process path [2]. In a recent review of modern QRPA calculations of β-decay rates for astrophysical applications [2], Borzov has emphasized the importance of performing calculations based on self-consistent mean-field models, rather than on empirical mean-field potentials, e.g., the Woods-Saxon potential. In a self-consistent framework both the nuclear ground states, i.e., the masses which determine the possible r-process path, and the corresponding β-decay properties are calculated from the same energy density functional or effective nuclear interaction. This approach ensures the consistency of the nuclear structure input for astrophysical modeling, and allows reliable extrapolations of the nuclear spin-isospin response to regions of very neutron-rich nuclei.

The fully consistent proton-neutron (PN) relativistic QRPA [3,4] has recently been employed in the calculation of β-decay half-lives of neutron-rich nuclei in the N≈50 and N≈82 regions [5]. The model is based on the relativistic QRPA [6], formulated in the canonical basis of the relativistic Hartree-Bogoliubov (RHB) framework [7]. The RHB+RQRPA model is fully self-consistent. For the interaction in the particle-hole channel modern effective Lagrangians with density-dependent meson-nucleon couplings are used, and pairing correlations are described by the pairing part of the finite range Gogny interaction. Both in the particle-hole (ph) and particle-particle (pp) channels, the same interactions are used in the RHB equations which determine the nuclear ground-state, and in the matrix equations of the RQRPA. This is important because the energy weighted sum rules are only satisfied if the pairing interaction is consistently included both in the static RHB and in the dynamical RQRPA calculations. In both channels the same strength parameters of the interactions are used in the RHB and RQRPA calculations. The formulation of the RHB+RQRPA model in the canonical quasiparticle basis enables the description of weakly-bound neutron-rich nuclei far from stability, because this basis diagonalizes the density matrix and includes both the bound states and the positive-energy single-particle continuum [6].

In the corresponding proton-neutron RQRPA [3,4] the spin-isospin-dependent interaction terms are generated by the π- and ρ-meson exchange. Although the direct one-pion contribution to the nuclear ground state vanishes at the mean-field level because of parity conservation, it must be included in the calculation of spin-isospin excitations. In addition, the derivative type of the pion-nucleon coupling necessitates the inclusion of the zero-range Landau-Migdal term, which accounts for the contact part of the nucleon-nucleon interaction, with the strength parameter g' adjusted to reproduce experimental data on the excitation energies of Gamow-Teller resonances (GTR). The model also includes the $T = 0$ proton-neutron pairing interaction: a short-range repulsive Gaussian function combined with a weaker longer-range attractive Gaussian [8]. In general the calculated β-decay half-lives are very sensitive to the strength of the $T = 0$ pairing which, in the case of β^--decay, enhances the Gamow-Teller strength in the Q_{β^-} energy window.

Standard relativistic mean-field models are based on the static approximation, i.e., the nucleon self-energy is real, local, and energy-independent. Consequently, these models describe correctly the ground-state properties and the sequence of single-particle levels in finite nuclei, but not the level density around the Fermi surface. The reason is the low effective nucleon mass m^* which, in the relativistic framework, is also related to the Dirac mass $m_D = m + S(\boldsymbol{r})$, where m is the bare nucleon mass and $S(\boldsymbol{r})$ denotes the scalar nucleon self-energy, and thus constrained by the empirical spin-orbit energy splittings. The difference between the vector and scalar nucleon self-energies determines the spin-orbit potential, whereas their sum defines the effective single-nucleon potential, and is constrained by the nuclear matter binding energy at saturation density. The energy spacings between spin-orbit partner states in finite nuclei, and the nuclear matter binding and saturation, place the following constraints on the values of the Dirac mass and the nucleon effective mass: $0.55\,m \leqslant m_D \leqslant 0.6\,m$, $0.64\,m \leqslant m^* \leqslant 0.67\,m$, respectively. These values have been used in most standard relativistic mean-field effective interactions. However, when these interactions are used in the calculation of β^- decay rates, the resulting half-lives are usually more than an order of magnitude longer than the empirical values. This is because the low effective nucleon mass implies a low density of states around the Fermi surface, and therefore in a self-consistent relativistic QRPA calculation of β-decay the transition energies will be low, resulting in long lifetimes. In order to reproduce the empirical half-lives, it is thus necessary to employ relativistic effective interactions with higher values of the nucleon effective mass. We note that in the case of nonrelativistic global effective interactions such as, for instance, Skyrme-type interactions, calculation of ground-state properties and excitation energies of quadrupole giant resonances have shown that a realistic choice for the nucleon effective mass is in the interval $m^*/m = 0.8 \pm 0.1$ [9,10].

In Ref. [5] we have used the RHB+RQRPA model to calculate β-decay half-lives of neutron-rich nuclei in the $N \approx 50$ and $N \approx 82$ regions. Starting from the standard density-dependent effective interaction DD-ME1 [11] ($m_D = 0.58\,m$, $m^* = 0.66\,m$), a new effective interaction was adjusted with higher values for the Dirac mass and the nucleon effective mass: $m_D = 0.67\,m$, $m^* = 0.76\,m$. However, a standard RMF interaction with such a high value of the Dirac mass would systematically underestimate the empirical spin-orbit splittings in finite nuclei. To compensate the reduction of the effective spin-orbit potential caused by the increase of the Dirac mass, the DD-ME1 interaction was further extended by including an additional interaction term: the tensor coupling of the ω-meson to the nucleon. The resulting interaction was used in the relativistic Hartree-Bogoliubov calculation of nuclear ground states. With the Gogny D1S interaction in the $T = 1$ pairing channel, and also including the $T = 0$ particle-particle interaction in the PN-QRPA, it was possible on one hand to reproduce the empirical values of the energy spacings between spin-orbit partner states in spherical nuclei, and on the other hand the calculated β-decay half-lives were in reasonable agreement with the experimental data for the Fe, Zn, Cd, and Te isotopic chains.

With the model developed in Ref. [5] the problems of the low effective mass and long β-decay half-lives were solved on an ad hoc basis. The effective interaction was adjusted with the particular purpose of increasing the effective nucleon mass, and the resulting problem of the reduction of the effective spin-orbit potential was solved by the inclusion of an additional interaction term. A much better solution is provided by the recently introduced relativistic mean-field model with momentum-dependent nucleon self-energies [12,13]. In this model the standard effective Lagrangian with density-dependent meson-nucleon coupling vertices is extended by including a particular form of the couplings between the isoscalar meson fields and the derivatives of the nucleon fields. This leads to a linear momentum dependence of the scalar and vector self-energies in the Dirac equation for the in-medium nucleon. Even though the extension of the standard mean-field framework is phenomenological, it is nevertheless based on Dirac-Brueckner calculations of in-medium nucleon self-energies, and consistent with the relativistic optical potential in nuclear matter, extracted from elastic proton-nucleus scattering data. In the extended model it is possible to increase the effective nucleon mass, while keeping a small Dirac mass which is required to reproduce the empirical strength of the effective spin-orbit potential.

In the very recent work of Ref. [13], in particular, an improved Lagrangian density of the model with density-dependent and derivative couplings (D^{3}C) has been introduced. The parameters of the coupling functions were adjusted to ground-state properties of eight doubly-magic spherical nuclei, and the results for nuclear matter, neutron matter, and finite nuclei were compared to those obtained with conventional RMF models. It was shown that the new effective interaction improves the description of binding energies, nuclear shapes and spin-orbit splittings of single-particle levels. More important, it was possible to increase the effective nucleon mass ($m^* = 0.71\,m$) and, correspondingly, the density of single-nucleon levels close to the Fermi surface as compared to standard RMF models. At the same time the Dirac mass was kept at the small value $m_D = 0.54m$, which ensures that the model reproduces the empirical spin-orbit splittings. The momentum dependence of the nucleon self-energies provides also a correct description of the empirical Schrödinger-equivalent central optical potential.

In this work we employ the model with density-dependent and derivative couplings (D^{3}C) of Ref. [13] in the calculation of β-decay rates of neutron-rich nuclei in several isotopic chains in the $Z \approx 28$ and $Z \approx 50$ regions. The results of fully consistent RHB plus proton-neutron QRPA will be compared with those obtained with the standard density-dependent RMF interaction DD-ME1 and, in addition, with a new effective interaction based on the D^3C model, but with an even higher value of the effective nucleon mass. We will analyze the dependence of the β-decay half-lives on the choice of the effective particle-hole interaction, and the strength of the $T = 0$ pairing interaction.

The functional forms of the density dependence of the σ, ω and ρ meson-nucleon couplings are identical for the conventional DD-ME1 effective interaction and the D^3C model. The latter includes momentum-dependent isoscalar scalar and vector self-energies, and thus contains two additional coupling functions Γ_S and Γ_V. In Ref. [13] these have been parametrized with the following functional form:

$$\Gamma_i(x) = \Gamma_i(\rho_{\rm ref})x^{-a_i} \quad \text{for} \quad i = S, V, \qquad (1)$$

where $x = \rho_v/\rho_{\rm ref}$, ρ_v is the vector density, and the reference density $\rho_{\rm ref}$ corresponds to the vector density determined at the saturation point of symmetric nuclear matter. In the parametrization of Ref. [13] $a_S = a_V = 1$, and we will retain these values in the following calculation. The parameters $\Gamma_S(\rho_{\rm ref})$ and $\Gamma_V(\rho_{\rm ref})$ have been constrained by the requirement that the resulting optical potential in symmetric nuclear matter at saturation density has the value 50 MeV at a nucleon energy of 1 GeV. In total there are 10 adjustable parameters in the D^3C model, compared to eight for the standard density-dependent RMF models, e.g., the DD-ME1 parametrization.

The effective nucleon mass of the D^3C model is $m^* = 0.71\,m$, compared to $m^* = 0.66\,m$ for DD-ME1. In addition, starting from D^3C, for the purpose of calculating β-decay rates we have adjusted a new parametrization with $m^* = 0.79\,m$, which is much closer to the effective masses used in nonrelativistic Skyrme effective interactions [9,10]. The new effective interaction which, for simplicity we denote D^3C^*, has been adjusted following the original procedure of Ref. [13], with an additional constraint on the effective nucleon mass. Even though we have tried to increase the effective mass as much as possible, $m^* = 0.79\,m$ is the highest value for which a realistic description of nuclear matter and finite nuclei is still possible, and the quality of the calculated nuclear matter equation of state and of ground-state properties of spherical nuclei is comparable to that of the DD-ME1 and D^3C interactions. The three interactions are compared in Table I, where we include the characteristics of the corresponding nuclear matter equations of state at saturation point: the saturation density $\varrho_{\rm sat}$, the binding energy per particle a_V, the symmetry energy a_4, the nuclear matter compression modulus K_∞, the Dirac mass m_D, and the effective (Landau) mass m^*. In addition, for the two interactions with energy-dependent single-nucleon potentials, we compare the values of $\Gamma_S(\rho_{\rm ref})$ and $\Gamma_V(\rho_{\rm ref})$. We notice a pronounced increase of the strength of the scalar field. This is, however, compensated by the corresponding decrease of the strength of the vector coupling, so that the difference $\Gamma_V(\rho_{\rm ref}) - \Gamma_S(\rho_{\rm ref})$ is practically the same for D^3C and D^3C^*. For both interactions the optical potential at 1 GeV nucleon energy has been constrained to 50 MeV. With the increase of the effective nucleon mass from DD-ME1 to D^3C and D^3C^*, we also note the corresponding decrease of the nuclear matter compression modulus K_∞. This correlation between K_∞ and m^* is also well known in nonrelativistic Skyrme effective interactions [10].

TABLE I. Properties of symmetric nuclear matter at saturation density calculated with the models DD-ME1, D^3C, and D^3C^*.

	DD-ME1	D^3C	D^3C^*
$\varrho_{\rm sat}$ [fm^{-3}]	0.152	0.151	0.152
a_V [MeV]	−16.20	−15.98	−16.30
a_4 [MeV]	33.1	31.9	33.0
K_∞ [MeV]	244.5	232.5	224.9
m_D/m	0.58	0.54	0.57
m^*/m	0.66	0.71	0.79
Γ_S	0.0	−21.632	−146.089
Γ_V	0.0	302.188	180.889

In Fig. 1 we display the neutron and proton single-particle levels in ^{132}Sn calculated in the relativistic mean-field model with the DD-ME1, D^3C, and D^3C^* effective interactions, in comparison with available data for the levels close to the Fermi surface [14]. Compared to the DD-ME1 interaction, the enhancement of the effective mass in D^3C and D^3C^* results in the increase of the density of states around the Fermi surface, and the calculated spectra are in much better agreement with the empirical energy spacings.

In the next step the three effective interactions have been tested and compared in RHB plus proton-neutron relativistic QRPA calculations of β-decay half-lives for the isotopic chains: Fe, Ni, Zn, Cd, Sn and Te. The nuclear ground-states have been calculated in the RHB model with the DD-ME1, D^3C, and D^3C^* effective interactions in the particle-hole channel, and the pairing part of the Gogny force,

$$V^{pp}(1,2) = \sum_{i=1,2} e^{-((\mathbf{r}_1-\mathbf{r}_2)/\mu_i)^2} \times (W_i + B_i P^\sigma - H_i P^\tau - M_i P^\sigma P^\tau) \qquad (2)$$

in the particle-particle channel, with the set D1S [15] for the parameters μ_i, W_i, B_i, H_i and M_i $(i = 1, 2)$. This force has been very carefully adjusted to pairing properties of finite nuclei all over the periodic table. In particular, the basic advantage of the Gogny force is the finite range, which automatically guarantees a proper cut-off in momentum space. In the following calculations we have also used the Gogny interaction in the $T = 1$ pp-channel of the PN-RQRPA.

The RHB ground-state solution determines the single-nucleon canonical basis, i.e., the configuration space in which the matrix equations of the relativistic QRPA are expressed (see Refs. [4,6] for a detailed presentation of the formalism). The particle-hole residual interaction of the PN-RQRPA is derived from the following Lagrangian density:

$$\mathcal{L}^{\rm int}_{\pi+\rho} = -g_\rho \bar{\psi}\gamma^\mu \vec{\rho}_\mu \vec{\tau}\psi - \frac{f_\pi}{m_\pi}\bar{\psi}\gamma_5\gamma^\mu \partial_\mu \vec{\pi}\vec{\tau}\psi. \qquad (3)$$

The coupling between the ρ-meson and the nucleon is already contained in the RHB effective Lagrangian, and the same interaction is consistently used in the isovector channel of the QRPA. The direct one-pion contribution to the ground-state RHB solution vanishes because of parity-conservation, but it must be included in the calculation of the Gamow-Teller

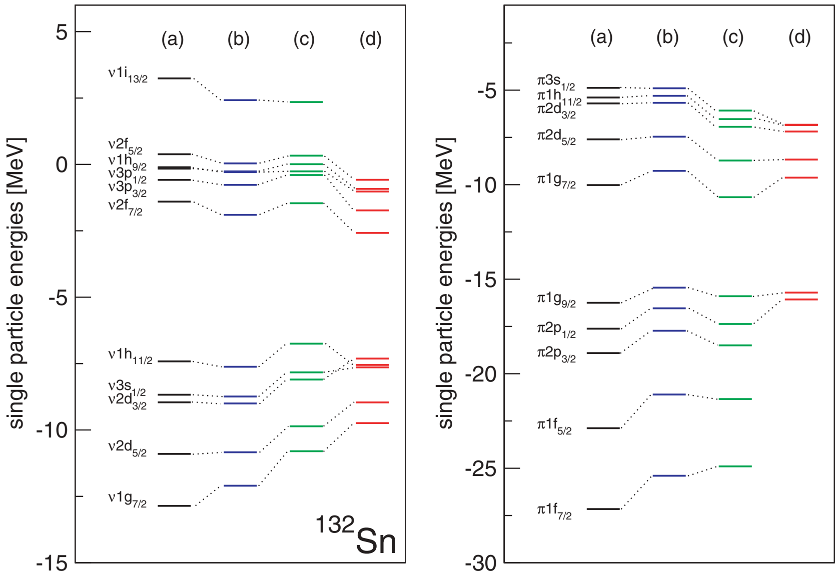

FIG. 1. (Color online) Neutron (left panel) and proton (right panel) single-particle levels in ^{132}Sn calculated with the DD-ME1 (a), D^{3}C (b), and D^{3}C* (c) interactions, compared to experimental levels (d) [14].

strength. For the pseudovector pion-nucleon coupling we have used the standard values:

$$m_\pi = 138.0 \text{ MeV}, \quad \frac{f_\pi^2}{4\pi} = 0.08. \tag{4}$$

In addition, the zero-range Landau-Migdal term accounts for the contact part of the isovector channel of the nucleon-nucleon interaction

$$V_{\delta\pi} = g' \left(\frac{f_\pi}{m_\pi}\right)^2 \vec{\tau}_1\vec{\tau}_2 \boldsymbol{\Sigma}_1 \cdot \boldsymbol{\Sigma}_2 \delta(\boldsymbol{r}_1 - \boldsymbol{r}_2). \tag{5}$$

For each effective interaction, the strength parameter g' is adjusted to reproduce the excitation energy of the Gamow-Teller resonance in ^{208}Pb. In the present calculation these values are $g' = 0.55$, 0.54 and 0.76, for DD-ME1, D^{3}C, and D^{3}C*, respectively.

Finally, the proton-neutron QRPA interaction is completely determined by the choice of the $T = 0$ pairing interaction [8]:

$$V_{12} = -V_0 \sum_{j=1}^{2} g_j \, e^{-r_{12}^2/\mu_j^2} \, \hat{\Pi}_{S=1,T=0}, \tag{6}$$

where $\hat{\Pi}_{S=1,T=0}$ projects onto states with $S = 1$ and $T = 0$. The ranges $\mu_1 = 1.2$ fm and $\mu_2 = 0.7$ fm of the two Gaussians are the same as for the Gogny interaction Eq. (2), and the relative strengths $g_1 = 1$ and $g_2 = -2$ are adjusted so that the force is repulsive at small distances. The only remaining free parameter is V_0, the overall strength.

The half-life of the β^--decay of an even-even nucleus in the allowed Gamow-Teller approximation is calculated from the following expression:

$$\frac{1}{T_{1/2}} = \sum_m \lambda_{if}^m = D^{-1} g_A^2 \sum_m \int dE_e \left| \sum_{pn} \langle 1_m^+ || \boldsymbol{\sigma}\tau_- || 0^+ \rangle \right|^2 \frac{dn_m}{dE_e}, \tag{7}$$

where $D = 6163.4 \pm 3.8$ s [16]. $|0^+\rangle$ denotes the ground state of the parent nucleus, and $|1_m^+\rangle$ is a state of the daughter nucleus. The sum runs over all final states with an excitation energy smaller than the Q_{β^-}-value. In order to account for the universal quenching of the Gamow-Teller strength function, we have used the effective weak axial nucleon coupling constant $g_A = 1$, instead of $g_A = 1.26$ [17]. The kinematic factor in Eq. (7) can be written as

$$\frac{dn_m}{dE_e} = E_e \sqrt{E_e^2 - m_e^2} (\omega - E_e)^2 F(Z, A, E_e), \tag{8}$$

where ω denotes the energy difference between the initial and the final state. The Fermi function $F(Z, A, E_e)$ corrects the phase-space factor for the nuclear charge and finite nuclear size effects [18].

In Fig. 2 we display the β^--decay half-lives of iron, nickel, and zinc isotopes calculated with the DD-ME1, D^{3}C, and D^{3}C*, and compare them with the experimental values taken from NUDAT database [19]. The data for ^{76}Ni and ^{78}Ni are from Ref. [20]. Open symbols correspond to values calculated without the inclusion of $T = 0$ pairing. Since the β^--decay rates are generally very sensitive to the proton-neutron pairing, and its strength is usually adjusted separately for each isotopic chain, we will first discuss the results obtained without the $T = 0$ pairing interaction. For all three isotopic chains, the shortest half-lives are obtained with the interaction with the highest effective mass, i.e. D^{3}C*, even though these are still far from the experimental values. For the Fe nuclei all three interactions give similar results, whereas more pronounced differences are found for the Ni and Zn isotopic chains. In the two latter cases similar results are obtained with DD-ME1 and D^{3}C and, in fact, longer half-lives are predicted by D^{3}C, even though it has a higher effective nucleon mass. Much shorter half-lives for the Ni and Zn nuclei are calculated with the D^{3}C* effective interaction. The origin of these large differences in the calculated rates can be understood from Table II, where we list the transition energies for the strongest transition in the Zn isotopes with $76 \leqslant A \leqslant 82$: $\nu 2p_{1/2} \to \pi 2p_{3/2}$. We note that the transition energies for the DD-ME1 and D^{3}C interactions are

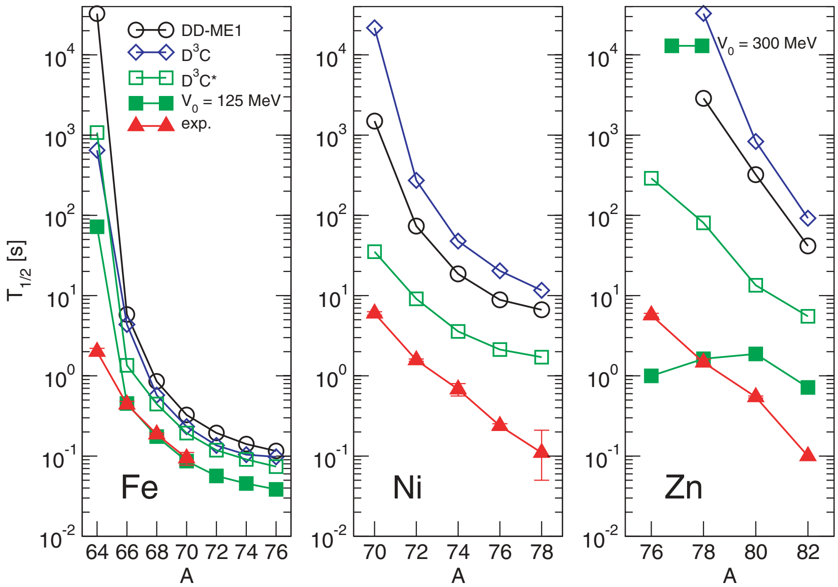

FIG. 2. (Color online) β-decay half-lives of Fe (left panel), Ni (middle panel), and Zn (right panel) nuclei, calculated with the DD-ME1, D^{3}C, and D^{3}C* effective interactions, compared with the experimental values [19]. Open symbols correspond to PN-QRPA values calculated without the inclusion of the $T = 0$ pairing interaction. The filled squares are half-lives calculated with the D^{3}C* interaction and $T = 0$ pairing, with the strength parameter $V_0 = 125$ MeV for Fe, and $V_0 = 300$ MeV for Zn isotopes.

comparable and, in particular, those calculated with DD-ME1 are slightly larger, resulting in faster β^--decay rates. Both interaction predict a β-stable ^{76}Zn. On the other hand, the transition energies predicted by the interaction D^{3}C* are much larger and, correspondingly, the calculated half-lives are at least an order of magnitude shorter.

A similar situation is found in the neutron-rich nuclei in the $Z \approx 50$ region. The calculated half-lives of Cd, Sn, and Te nuclei are plotted in Fig. 3, in comparison with available data [19]. The Cd isotopes, in particular, are calculated as β-stable with the D^{3}C interaction, because the predicted transition energies are smaller than the electron rest mass. Much better results are obtained with the modified interaction D^{3}C*, which clearly reproduces the isotopic trend of the half-lives of neutron-rich Cd nuclei. DD-ME1 and D^{3}C produce almost identical results for Sn and Te nuclei. Shorter half-lives, especially for Sn, are calculated with D^{3}C*, but these are still orders of magnitude from the experimental values. It appears that all three interactions reproduce the isotopic trend in the Te chain.

We have considered the effect of the $T = 0$ pairing interaction on the calculated β-decay half-lives only for the D^{3}C* effective interaction which, with the effective nucleon mass $m^*/m = 0.79$ comparable to those of nonrelativistic effective interactions, gives the shortest half-lives. Even without the inclusion of the proton-neutron pp interaction, for the Fe nuclei the calculated half-lives are already close to the experimental values, except for ^{64}Fe (see Fig. 2). By adjusting the value of the strength parameter of the $T = 0$ pairing to $V_0 = 125$ MeV, the PN-QRPA calculation reproduces the β-decay half-lives of ^{66}Fe, ^{68}Fe and ^{70}Fe (filled squares). In the case of Ni isotopes the $T = 0$ interaction in the pp-channel is not effective because of the $Z = 28$ and $N = 40$ closures [5,8]. The $\pi 1 f_{7/2}$ orbit is completely occupied, and the transition $\nu 1 f_{5/2} \to \pi 1 f_{7/2}$ is thus blocked. The $T = 0$ pairing could only have an effect on the $\nu 1 g_{9/2} \to \pi 1 g_{9/2}$ transition, but the $\pi 1 g_{9/2}$ orbital is located high above the Fermi surface. Thus the $T = 0$ pp interaction cannot shift the low-energy GT strength and enhance the β-decay rates. Even using the D^{3}C* interaction, the calculated half-lives are an order of magnitude longer than the experimental values.

The principal advantage of the self-consistent approach to the modeling of β-decay rates is the use of universal (A independent) interactions in the ph-channel and, in many cases including the model used in this work, in the $T = 1$ pp-channel. Unfortunately, this is not possible in the $T = 0$ pp-channel, for which no information is contained in the ground-state data. The strength of this interaction is adjusted separately for each isotopic chain or, in the best case, a single value of the strength can be used in a certain mass region [5,8]. It is especially difficult to keep the same strength of the $T = 0$ pairing when crossing a closed shell. Thus in going from the Fe to the Zn isotopic chain we had to increase the strength parameter V_0 by more than a factor two. The value $V_0 = 300$ MeV has been adjusted to reproduce the half-life of ^{78}Zn (filled squares in the right panel of Fig. 2) but, even though the calculated values are in qualitative agreement with the data, with the inclusion of the $T = 0$ pairing the PN-QRPA results do not reproduce the isotopic dependence of the experimental half-lives. In other words, it was not possible to find a single value of the proton-neutron pairing strength that could reproduce the half-lives of neutron-rich Zn isotopes.

The filled squares in Fig. 3 correspond to the half-lives calculated with the D^{3}C* effective interaction, the $\pi + \rho$ plus Landau-Migdal interaction in the ph-channel, the Gogny

TABLE II. Transition energies (in MeV) for the strongest transition in the Zn isotopes: $\nu 2p_{1/2} \to \pi 2p_{3/2}$.

	DD-ME1	D^{3}C	D^{3}C*
^{76}Zn	0.15	−0.05	1.74
^{78}Zn	0.93	0.72	2.65
^{80}Zn	2.01	1.80	3.69
^{82}Zn	2.69	2.51	4.58

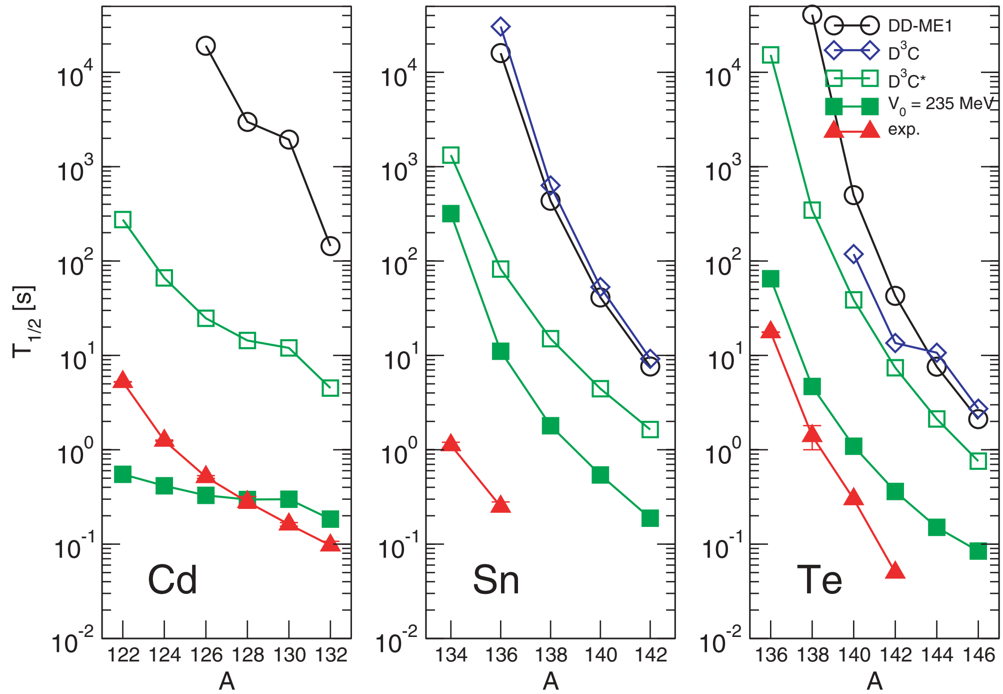

FIG. 3. (Color online) Same as in Fig. 2, but for the Cd (left panel), Sn (middle panel), and Te (right panel) isotopic chains. For the D^3C^* effective interaction, in all three isotopic chains the strength of the $T = 0$ pairing interaction is $V_0 = 235$ MeV (filled squares).

interaction Eq. (2) in the $T = 1$ *pp*-channel, and the $T = 0$ pairing Eq. (6). The strength of the latter: $V_0 = 235$ MeV, has been adjusted to the half-life of ^{128}Cd, and this value has been used for the Cd, Sn and Te isotopic chains. The effect of the $T = 0$ pairing is especially pronounced for Cd and Te nuclei, and the results are in qualitative agreement with the available data, although the calculation does not reproduce the isotopic trend for the Cd chain, and overestimates the half-lives of Te isotopes. On the other hand, for the proton closed-shell Sn nuclei the $T = 0$ pairing interaction is much less effective, and the calculated half-lives of ^{134}Sn and ^{136}Sn are two orders of magnitude longer than the experimental values. Better results could be obtained, of course, by adjusting V_0 separately for each isotopic chain.

The calculations performed in this work have shown that the extension of the standard relativistic mean-field framework to include momentum-dependent (energy-dependent in stationary systems) nucleon self-energies naturally leads to an enhancement of the effective (Landau) nucleon mass, and thus to an improved PN-QRPA description of β^--decay rates. However, even though the momentum-dependent RMF model with density-dependent meson-nucleon couplings, adjusted here to $m^* = 0.79\,m$, predicts half-lives of neutron-rich medium-mass nuclei in qualitative agreement with data, the results are not as good as those obtained in the most advanced non-relativistic self-consistent density-functional plus continuum-QRPA calculations [2,21,22], or with the self-consistent HFB+QRPA model with Skyrme interactions of Ref. [8]. Namely, although we have been able to increase the effective mass of the interaction used in the RHB calculations of nuclear ground states to $m^* = 0.79\,m$, a value which is sufficient for the description of giant resonances [9,10], the detailed description of the low-energy Gamow-Teller strength necessitates an even higher value of m^*. In fact, the effective mass of the Skyrme SkO' interaction used in Ref. [8] is $m^* = 0.9\,m$, whereas the continuum-QRPA calculations by Borzov are based on the Fayans phenomenological density functional with the bare nucleon mass, i.e., $m^* = m$ [2,21,22]. However, it would be very difficult to further increase the effective nucleon mass in the framework of the model used in this work, i.e., on the nuclear matter level, without destroying the good agreement with empirical ground-state properties of finite nuclei. On the other hand, this would not even be the correct procedure because the additional enhancement of the effective nucleon mass is due to the coupling of single-nucleon levels to low-energy collective vibrational states, an effect which goes entirely beyond the mean-field approximation and is not included in the present model. In principle, the effect of two- and three-phonon states on the weak-interaction rates could be taken into account by explicitly considering the coupling of single-quasiparticle states to phonons, and the resulting complex configurations would certainly lead to a redistribution of low-energy Gamow-Teller strength. Even though such extended (second) RPA approaches have been routinely used for many years in the calculation of widths of isoscalar and isovector giant resonances, no systematic large-scale calculations of β-decay rates have been reported so far. We have therefore started to develop a new self-consistent model based on the recently introduced covariant theory of particle-vibration coupling [23], and this framework will be applied in the calculation of β-decay half-lives of neutron-rich medium mass nuclei.

In heavier nuclei, or in nuclei with an even higher neutron to proton asymmetry, in addition to allowed Gamow-Teller transitions, first-forbidden transitions must be taken into account in the calculation of β-decay half-lives. As it has been shown in recent studies by Borzov using the density-functional plus continuum-QRPA framework [2,21,22], the first-forbidden decays have a pronounced effect on the β-decay characteristics of r-process nuclei in the $Z \approx 28$, $N > 50$; $Z \geqslant 50$, $N > 82$; and $Z = 60$–70, $N \approx 126$ regions. For studies of weak-interaction rates in r-process nuclei very far from stability, it will therefore be important to include first-forbidden transitions in the relativistic PN-QRPA model.

ACKNOWLEDGMENTS

This work has been supported in part by the Bundesministerium für Bildung und Forschung-project 06 MT 246, by the Gesellschaft für Schwerionenforschung GSI-project TM-RIN. T.M. and D.V. would like to acknowledge the support from the Alexander von Humboldt-Stiftung.

[1] K. Langanke and G. Martínez-Pinedo, Rev. Mod. Phys. **75**, 819 (2003).
[2] I. N. Borzov, Nucl. Phys. **A777**, 645 (2006).
[3] D. Vretenar, N. Paar, T. Nikšić, and P. Ring, Phys. Rev. Lett. **91**, 262502 (2003).
[4] N. Paar, T. Nikšić, D. Vretenar, and P. Ring, Phys. Rev. C **69**, 054303 (2004).
[5] T. Nikšić, T. Marketin, D. Vretenar, N. Paar, and P. Ring, Phys. Rev. C **71**, 014308 (2005).
[6] N. Paar, P. Ring, T. Nikšić, and D. Vretenar, Phys. Rev. C **67**, 034312 (2003).
[7] D. Vretenar, A. V. Afanasjev, G. A. Lalazissis, and P. Ring, Phys. Rep. **409**, 101 (2005).
[8] J. Engel, M. Bender, J. Dobaczewski, W. Nazarewicz, and R. Surman, Phys. Rev. C **60**, 014302 (1999).
[9] P.-G. Reinhard, Nucl. Phys. **A649**, 305c (1999).
[10] E. Chabanat, P. Bonche, P. Haensel, J. Meyer, and R. Schaeffer, Nucl. Phys. **A627**, 710 (1997); **A635**, 231 (1998).
[11] T. Niksić, D. Vretenar, P. Finelli, and P. Ring, Phys. Rev. C **66**, 024306 (2002).
[12] S. Typel, T. v. Chossy, and H. H. Wolter, Phys. Rev. C **67**, 034002 (2003).
[13] S. Typel, Phys. Rev. C **71**, 064301 (2005).
[14] V. I. Isakov, K. I. Erokhina, H. Mach, M. Sanchez-Vega, and B. Fogelberg, Eur. Phys. J. A **14**, 29 (2002).
[15] J. F. Berger, M. Girod, and D. Gogny, Comput. Phys. Commun. **63**, 365 (1991).
[16] I. N. Borzov and S. Goriely, Phys. Rev. C **62**, 035501 (2000).
[17] A. Bohr and B. R. Mottelson, *Nuclear Structure* (Benjamin, New York, 1975), Vol. II.
[18] E. J. Konopinski and M. E. Rose, in *α-, β-, and γ-ray Spectroscopy*, edited by K. Siegbahn (North-Holland Pub. Co., Amsterdam, 1965), p. 1327.
[19] NUDAT database, National Nuclear Data Center, http://www.nndc.bnl.gov/nndc/nudat/
[20] P. T. Hosmer *et al.*, Phys. Rev. Lett. **94**, 112501 (2005).
[21] I. N. Borzov, Phys. Rev. C **67**, 025802 (2003).
[22] I. N. Borzov, Phys. Rev. C **71**, 065801 (2005).
[23] E. Litvinova and P. Ring, Phys. Rev. C **73**, 044328 (2006).